Fixed-Time Disturbance Observer-Based Power Control of Wave Power Generation System

Chao Bai[1] and Ning Wang[2(✉)]

[1] School of Marine Electrical Engineering, Dalian Maritime University, Dalian, China

[2] School of Marine Engineering, Dalian Maritime University, Dalian, China
n.wang.dmu.cn@gmail.com

Abstract. In this paper, the current tracking control problem of direct-drive wave power generation system disturbed by complex environment is solved by designing finite-time controller(FTC) and backstepping sliding mode controller (BSMC). In order to realize the maximum power tracking control of the directly driven wave energy converter (DWEC), a fixed-time observer (FTDO) is designed to quickly compensate for environmental disturbances, and a backstepping sliding mode control strategy based on FTDO (FTDO-BSMC) is proposed to accurately track the current. Finally, Numerical simulation and comparison demonstrate the feasibility and superiority of the proposed scheme.

Keywords: direct-drive wave energy conversion · maximum wave energy tracking · fixed-time disturbance observer · back-stepping sliding mode control

1 Introduction

In recent years, the problem of energy shortages has become increasingly prominent, and the ocean contains huge amounts of energy. The low energy absorption efficiency of wave energy converters (WECs) has become a bottleneck problem in promotion and application [1–3]. As a type of wave energy power generation device, Permanent magnet linear generator (PMLG) is used to directly convert the moving wave energy into electrical energy [4]. Compared with other forms of multi-stage conversion links, it reduces power loss and improves the wave energy of the entire device. At present, in order to improve the efficiency of wave energy, researchers have carried out maximum power control research. Through mechanical control or electrical control, the wave energy conversion system can resonate with waves.

Supported by organization National Natural Science Foundation of China (Grant 52271306) Innovative Research Foundation of Ship General Performance (Grant 31422120).

H. R. Karimi and N. Wang (Eds.): S-Cube 2022, LNICST 487, pp. 133–145, 2023.
https://doi.org/10.1007/978-3-031-34899-0_9

Two classical theories of amplitude-phase control and complex-conjugate control for power control of wave power generation. In the amplitude-phase control, the motion of the floating body and the wave must meet certain amplitude and phase conditions to reach the resonance state and improve the output power [5–8]. However, in this control method, the natural frequency of the system is related to the wave period. For the actual sea state, it is difficult to always meet the phase condition of reaching the resonance state, and the applicability is poor when the wave frequency bandwidth changes greatly. It is suitable for wave Sea conditions with a unique dominant frequency and a small frequency variation range. In complex conjugate control, the system damping force is related to the speed and displacement of the floating body, which can be divided into two parts: linear damping force and elastic damping force. The optimal velocity of the floating body can be obtained when the system damping is equal to the conjugate of the impedance within the WEC system. At this time, the floating body motion phase and the wave motion phase still differ by 90°. The system dynamics model is equivalent to the second-order resonant circuit of inductance-capacitance-resistance, and the response form of the system is similar to the series resonance of the resonant circuit [9]. However, when it is constrained by the system motion stroke, force and output power limit, its practicality is poor in the sea area with high wave energy density and frequent sea state changes. The hill-climbing method has a simple structure and few system model parameters, so it is also used in wave power generation systems [10,11]. However, the control response speed of the hill-climbing method is greatly affected by the inertia of the system, and the disturbance step size is not easy to select. If the step size is too large, oscillation will occur near the maximum power point, resulting in energy loss. If the step size is too small, the arrival speed will be too slow, which will affect the dynamic performance of the system, so it needs to be improved. In [12–14] , a control method of changing the disturbance step size is proposed. In the case of sudden wave changes, the variable step length control method can effectively improve the anti-jamming capability of the maximum power tracking of the system, and quickly re-tracking to near the maximum power point.

Nonlinear control and intelligent control have also been developed and applied in wave power generation systems with nonlinear and strong coupling. Model predictive control and neural network-based model predictive control have been widely used in wave power generation because they do not need to rely on accurate mathematical models [15–20]. However, there is still the problem of relying on historical data, and a large amount of ocean data needs to be obtained, which is constrained by the cost problem. Sliding mode control (SMC) can solve the state and input delay problems of the system very well [10,21,22]. However, nonlinear disturbances are ignored. For unknown disturbances, observers were used to improve control performance. In [23–25], considering the system state measurements and the state-dependent disturbances are not available for feedback purposes, an observer-based adaptive control strategy has been proposed. In [26–29] a finite-time disturbance observer is proposed, in which the disturbance of the system can be observed and compensated for in a finite time.

In this paper, the system dynamics model is combined with the linear motor kinematics model, the control model of the whole system is established, and a fixed-time disturbance observer (FTDO) is designed to quickly compensate for internal and external disturbances. Unlike the finite-time perturbation observer, the fixed-time observer does not depend on the initial observation error, and the observation effect is better. At the same time, a finite-time control strategy [30,31] and a fixed-time disturbance observer-based backstepping sliding-mode control strategy (FTDO-BSMC) are designed for the d-axis current and the q-axis current, respectively, to improve the anti-disturbance and response speed of the control system and achieve the maximum wave can be captured.

2 Preliminaries and Problem Description

2.1 Lemma

Lemma 1. The following system:

$$\dot{x}(t) = f(x(t)) \tag{1}$$

where f(·)is continuous and f(0)=0

Suppose there is a positive definite function V satisfies:

$$V + kV^{\alpha} \leq 0 \tag{2}$$

where $k > 0$ and $\alpha \in (0, 1)$,then the system(1) is stable in finite time.

Lemma 2. If there is a continuous radially bounded function V satisfies:

1) $\mathrm{V}(x) = 0 \Leftrightarrow x = 0$,
2) For any $x(t)$ can satisfy the inequality $\dot{V}(x) \leq -\gamma_1 \mathrm{V}^{\alpha}(x) - \gamma_2 \mathrm{V}^{\beta}(x)$, where γ_1, γ_2 , α and β. are all positive constants,and $0 < \alpha < 1, \beta > 1$, then the original system can converge to zero in a fixed time, and the convergence time T satisfies:

$$T \leq T_{\max} = \frac{1}{\gamma_1 (1 - \alpha)} + \frac{1}{\gamma_2 (\beta - 1)} \tag{3}$$

It can be seen from the above formula that the convergence time of the system is only related to the system parameters γ_1, γ_2, α and β.

2.2 Problem Description

The float of the direct-drive wave energy conversion (DWEC) moves with the waves and uses the linear generator to collect wave energy. Due to the special structure of the linear generator, there is no intermediate energy conversion link, which can effectively improve the utilization rate of wave energy. However, the marine environment is relatively complex. Due to the effect of wind and waves on the float, it is difficult for the float to remain in a vertical state all the time, which will cause

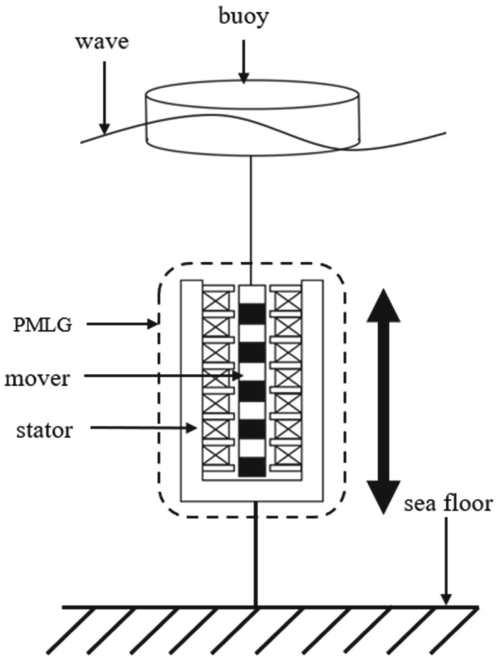

Fig. 1. Structure of direct-drive wave power generation device.

interference to the maximum wave energy tracking of DWEC. Therefore, an effective estimation of the interference is necessary to achieve accurate tracking of the maximum wave energy significant. Figure 1 shows the structure diagram of the direct-drive wave power generation device. Under the driving of the wave, the permanent magnet and the coil will produce relative motion to convert the mechanical energy of the wave into electrical energy.

The kinematic equation of the device is:

$$m\ddot{x} = F_e - F_g + F_r + F_b - mg \tag{4}$$

where m is the mass of the DWEC system, x is the mover displacement in the vertical direction, F_e is the wave excitation force, F_g is the anti-electromagnetic force of the linear motor, F_r and F_b are the radiation force and the static buoyancy of the float, respectively, which are expressed as:

$$F_r = -m_a\ddot{x} - R_a\dot{x} \tag{5}$$

$$F_b = -\kappa_1 x + mg \tag{6}$$

$$F_g = R_g\dot{x} + \kappa_2 x \tag{7}$$

Among them, m_a is the additional mass, R_a is the external damping, $\kappa_1 = \rho g S$ is the buoyancy coefficient, ρ is the seawater density, g is the gravitational acceleration, S is the contact surface between the float and the wave, R_g is the internal damping of the linear motor, and κ_2 is the elastic coefficient of the linear motor.

Combining (5)–(7), we have:

$$M\ddot{x} = F_e - (R_a + R_g)\dot{x} - (\kappa_1 + \kappa_2)x \tag{8}$$

where $M = m + m_a$ is the total mass of DWEC.

DWEC output power is:

$$P_g = \frac{F_e{}^2}{8R_a}\left(\left|1 - \frac{R_a - R_g - j(\omega M - \frac{\kappa}{\omega})}{R_a + R_g + j(\omega M - \frac{\kappa}{\omega})}\right|\right) \tag{9}$$

The modeling equations of device dynamics in two stationary coordinate systems are:

$$\begin{cases} \frac{di_d}{dt} = -\frac{R_s}{L_s}i_d + \frac{2\pi}{\lambda}vi_q - \frac{1}{L_s}u_d \\ \frac{di_q}{dt} = -\frac{R_s}{L_s}i_q - \frac{2\pi}{\lambda}vi_d + \frac{2\pi\psi_f}{\lambda L_s}v - \frac{1}{L_s}u_q \end{cases} \tag{10}$$

where i_d and i_q are the current components of the dq-axis, respectively.

The back electromagnetic force of the generator can also be expressed as:

$$F_g = 3\pi\frac{\psi_f i_q + (L_d - L_q)\, i_d i_q}{2\lambda} \tag{11}$$

where L_d and L_q are the inductances of the dq-axis, respectively.

It can be seen from the above formula that the anti-electromagnetic force F_g can be changed by changing the current component of the dq-axis. Therefore, the DWEC control model can be constructed by taking into account the unknown disturbances Δ existing in the actual marine environment and combining the dynamic and kinematic equations.

Combined with (8)–(11), the control model of the entire DWEC system is:

$$\begin{cases} \dot{i}_d = -\ell_s i_d + \alpha_2 v i_q - \frac{1}{L_s}u_d \\ \dot{x} = v \\ \dot{v} = D_1 + D_2 + \frac{\alpha_1\left(\psi_f + \ell_{dq}\dot{i}_d\right)i_q}{M} + \Delta \\ \dot{i}_q = -\ell_s i_q - \alpha_2 v i_d + \frac{\alpha_2}{L_s}\psi_f v - \frac{1}{L_s}u_q \end{cases} \tag{12}$$

where v is the mover speed of the linear motor, $D_1 = -\frac{R_a}{M}v - \frac{\kappa_1}{M}x, D_2 = \frac{F_e}{M}, \alpha_1 = \frac{3\pi}{2\lambda}, \ell_{dq} = L_d - L_q, \ell_s = \frac{R_s}{L_s}$.

3 Power Control System Design

3.1 Disturbance Observer Design

To design the observer, first define the variable $D = v_f - \chi$,

$$\begin{aligned} &\dot{\chi} = \lambda_1 D + \lambda_2 D^{\alpha} + \lambda_3 D^{\beta} + \lambda_4 sign\,(D) - \\ &D_1 - D_2 - \frac{\alpha_1(\psi_f + \ell_{dq} i_d) i_q}{M} \end{aligned} \tag{13}$$

Among them, $\lambda_i \in \mathbf{R}$ (i=1,2,3,4) is the positive definite diagonal matrix to be designed, each element in matrix λ_4 satisfies $\lambda_4 \geq \delta$,α and β are positive numbers, satisfies: $0 < \alpha < 1, \beta > 1$.

According to (12) and (13), the derivative of D can be obtained by:

$$\begin{aligned}&\dot{D}=\dot{v}_f-\dot{\chi}\\&=D_1+D_2+\frac{\alpha_1(\psi_f+\ell_{dq}i_d)i_q}{M}+\Delta-\\&\lambda_1 D-\lambda_2 D^{\alpha}-\lambda_3 D^{\beta}-\lambda_4 sign\,(D)-D_1-D_2\\&-\frac{\alpha_1(\psi_f+\ell_{dq}i_d)i_q}{M}\\&=-\lambda_1 D-\lambda_2 D^{\alpha}-\lambda_3 D^{\beta}-\lambda_4 sign\,(D)+\Delta\end{aligned}\tag{14}$$

Choose $\hat{\Delta}$ as follows:

$$\hat{\Delta}=\lambda_1 D+\lambda_2 D^{\alpha}+\lambda_3 D^{\beta}+\lambda_4 sign\,(D)\tag{15}$$

Define the observation error $\tilde{\Delta}=\hat{\Delta}-\Delta$, and the specific expression is:

$$\begin{aligned}&\tilde{\Delta}=\hat{\Delta}-\Delta\\&=\lambda_1 D+\lambda_2 D^{\alpha}+\lambda_3 D^{\beta}+\lambda_4 sign\,(D)+\\&D_1+D_2+\frac{\alpha_1(\psi_f+\ell_{dq}i_d)i_q}{M}-\dot{v}_f\\&=\dot{\chi}-\dot{v}_f\\&=-\dot{D}\end{aligned}\tag{16}$$

It can be seen from (16) that if Π converges, $\tilde{\Delta}$ can be guaranteed to converge.

3.2 D-Axis Current Loop-Finite Time Controller

In order to improve the output power, the d-axis adopts the zero vector control method, and the sliding-mode control surface of the d-axis is designed as:

$$s_d=i_d+k_{id}x_e\tag{17}$$

where $k_{id}>0$, $x_e=x-x_d$ is the displacement error and x_d is the wave reference displacement.

The first derivative of the d-axis sliding mode control surface is:

$$\dot{s}_d=\dot{i}_d+k_{id}v_e\tag{18}$$

The d-axis voltage control law is designed as:

$$u_d=L_s(-\varsigma_s i_d+\gamma_2 v i_q+k_{id}v_e+\eta_1 sign(s_d))\tag{19}$$

where η_1 is the designed constant.

3.3 Q-Axis Current Loop - Backstepping Sliding Mode Controller

Combined with the q-axis current tracking system, the tracking error is defined as:

$$x_e=x-x_d, v_e=v-v_d\tag{20}$$

where x_d is the wave reference velocity and v_d is the wave reference velocity.

The current control law of the q-axis is designed by the backstepping method as:

$$\begin{cases} \dot{x}_e = v_e \\ \dot{v}_e = D_1 + D_2 + \frac{\alpha_1 \psi_f}{M} i_q - \dot{v}_d + \Delta \\ \dot{i}_q = -\ell_s i_q - \alpha_2 v i_d + \frac{\alpha_2}{L_s} \psi_f v - \frac{1}{L_s} u_q \end{cases} \tag{21}$$

$$i_q^* = -\frac{M}{\alpha_1 \psi_f} \left(D_1 + D_2 - \dot{v}_d + k_{iq} v_e + \Delta \right) \tag{22}$$

Substituting (22) into (21), the error dynamic equation is:

$$\begin{cases} \dot{x}_e = v_e \\ \dot{v}_e = D_1 + D_2 + \frac{\alpha_1 \psi_f}{M} i_q - \dot{v}_d + \Delta \\ \dot{i}_{qe} = -\ell_s i_q + \frac{\gamma_2}{L_s} \psi_f v - \frac{1}{L_s} u_q - \alpha_2 v i_d + \frac{M}{\alpha_1 \psi_f} \\ (\mathrm{D}_1 + D_2 - \dot{v}_d + k_{iq} v_e + \Delta) \end{cases} \tag{23}$$

where $i_{_q} = i_{_q}^* - i_{_q}$.

In order to eliminate the current tracking error, the sliding mode control surface is designed:

$$s_q = i_{qe} + x_e \tag{24}$$

For the q-axis current tracking error (23), an integral sliding mode control surface is designed:

$$s_q = i_{qe} + k_{s_q} \int_0^t x_e dt - \frac{M k_{iq}}{\gamma_1 \psi_f} x_e - k_2 \int_0^t i_{qe} dt \tag{25}$$

For the q-axis integral sliding mode control surface, the voltage control law of the integral sliding mode control surface is designed as:

$$\begin{aligned} u_q = & \frac{M L_s}{\alpha_1 \psi_f} (\mathcal{D}_1 + \mathcal{D}_2 - \dot{v}_d - k_{iq} v_e + \hat{\Delta}) - \ell_s L_s i_q - \\ & \alpha_1 L_s v_d i_d + \alpha_1 \psi_f v - k_{s_q} x_e + \frac{M k_{iq}}{\alpha_1 \psi_f} v_e - k_2 i_{eq} \\ & + L_s \eta_2 sign(s_q) \end{aligned} \tag{26}$$

4 Stability Analysis

Assumption 1 : Δ in (12) is bounded, and $||\Delta|| \leq \delta < \infty$, where δ is a known constant.

Theorem 1 : Under Assumption 1, the constructed disturbance observer can accurately estimate the unknown disturbance Δ within the stable time, and the estimation error is zero.

Proof: Choose the following Lyapunov function:

$$V_d = \frac{1}{2} D^T D \tag{27}$$

According to formula (12), the derivative of V_d can be obtained:

$$\begin{aligned}
&\dot{V}_d = D^T \dot{D} \\
&= D^T \left(-\lambda_1 D - \lambda_2 D^\alpha - \lambda_3 D^\beta - \lambda_4 sign\left(D\right) + \Delta\right) \leq \\
&-\lambda_1 \left(D^T D\right) - \lambda_2 \left(D^T D\right)^{\frac{\alpha+1}{2}} - \lambda_3 \left(D^T D\right)^{\frac{\beta+1}{2}} \leq \\
&-\lambda_{\min}\left(\lambda_2\right)\left(D^T D\right)^{\frac{\alpha+1}{2}} - \lambda_{\min}\left(\lambda_3\right)\left(D^T D\right)^{\frac{\beta+1}{2}} = \\
&-2^{\frac{\alpha+1}{2}}\lambda_{\min}\left(\lambda_2\right)\left(\tfrac{1}{2}D^T D\right)^{\frac{\alpha+1}{2}} - 2^{\frac{\beta+1}{2}}\lambda_{\min}\left(\lambda_3\right)\left(\tfrac{1}{2}D^T D\right)^{\frac{\beta+1}{2}} \\
&= -2^{\frac{\alpha+1}{2}}\lambda_{\min}\left(\lambda_2\right)\left(V_d\right)^{\frac{\alpha+1}{2}} - -2^{\frac{\beta+1}{2}}\lambda_{\min}\left(\lambda_2\right)\left(V_d\right)^{\frac{\beta+1}{2}}
\end{aligned} \tag{28}$$

According to Lemma 2, it can be seen that the system Π is globally stable in fixed time, and the convergence time satisfies:

$$T_0 \leq T_{\max} = \frac{2^{\frac{1-\alpha}{2}}}{\lambda_{\min}\left(\lambda_2\right)\left(1-\alpha\right)} + \frac{2^{\frac{1-\beta}{2}}}{\lambda_{\min}\left(\lambda_3\right)\left(\beta-1\right)} \tag{29}$$

According to the definition of V_d, when $t \geq T_0$, $V_d \equiv 0$, $\dot{V}_d \equiv 0$, $\dot{\Pi} \equiv 0$, then:

$$\hat{\Delta} = 0, t \geq T_0 \tag{30}$$

Theorem 2 : FTDO-BSMC considers the model (12) that satisfies the hypothesis 1. Under the action of the disturbance observer (15), control laws (22), (26), the unknown external disturbance to the system can be observed in a fixed time. At the same time, the error signals x_e, v_e, i_{qe} can be stabilized to zero, and the actual state can also track the expected value under the action of the controller.

Proof: The proof process is divided into two steps. First, it is proved that the d-axis current converges on the sliding mode surface in a finite time, and then it is proved that the displacement, velocity tracking error and q-axis current tracking error are after reaching the designed non-singular terminal sliding mode surface. Asymptotically stable converges to zero.

Step 1: For the d-axis current tracking control subsystem, choose the following Lyapunov function:

$$V_1 = \frac{1}{2}s_d^2 \tag{31}$$

Taking the derivative of the above formula, we can get:

$$\begin{aligned}
\dot{V}_1 &= s_d \dot{s}_d \\
&= s_d(-\ell_s i_d + \gamma_2 v i_q - \tfrac{1}{L_s}u_d)
\end{aligned} \tag{32}$$

Substituting the voltage control law (22) into the above formula, we can get:

$$\begin{aligned}
\dot{V}_1 &= s_d(-k_1 s_d - \eta_1 sign(s_d)) \\
&= -k_1 s_d^2 - \eta_1 \left|s_d\right|
\end{aligned} \tag{33}$$

According to Lemma 1, the tracking error of the d-axis current tracking system can converge to zero within a finite time.

Step 2: For the q-axis current tracking system, establish the following Lyapunov function:

$$V_2=\frac{1}{2}v_e^2+\frac{1}{2}s_q^2 \tag{34}$$

Taking the derivative of (32), we get:

$$\dot{V}_2=v_e\dot{v}_e+s_q\dot{s}_q \tag{35}$$

Step 3: Considering the entire DWEC maximum wave energy tracking control system, design the Lyapunov function:

$$V=V_1+V_2 \tag{36}$$

Combining the disturbance observer (15) and the control law (19), (22), we get:

$$\dot{V}=-\eta_1\left|s_d\right|-k_1s_d^2-k_{iq}v_e^2-k_2s_q^2-\eta_2\left|s_q\right| \tag{37}$$

It can be known from the above formula that $\dot{V}\leq 0$. According to Lyapunov stability theory and Barbalat's lemma, when $t\rightarrow\infty$, x_e and v_e converge to zero. The whole system is asymptotically stable under the FTDO-BSMC control scheme.

5 Simulation Studies

In order to verify the effectiveness and feasibility of the proposed control strategy, this paper uses the direct-drive wave power generation device in the literature [5] for simulation research.

Comparing with the equivalent circuit method and sliding mode control (SMC) to verify the effectiveness of the proposed control model and control scheme. This control scheme proposes a high-level control model. The traditional equivalent circuit method is used to obtain the ideal q-axis current value , and then the control process is transformed into a high-level model virtual control quantity for direct control, which is conducive to improving the accuracy of device control. The reference displacement of the direct-drive wave energy power generation device is as follows:

$$x_d=sin\left(0.2t+3\right)cos\left(0.5\mathrm{t}+8\right) \tag{38}$$

The unknown disturbance is:

$$\Delta=\frac{20\sin(\frac{2t}{3}+5)\cos 0.5t\cos(\frac{t}{3})}{M} \tag{39}$$

As shown in Fig. 2, the designed fixed-time disturbance observer can effectively estimate the unknown disturbance in the marine environment, improve the tracking performance and suppress the disturbance. As shown in Fig. 3, the designed d-axis finite-time controller has a faster response speed than SMC in

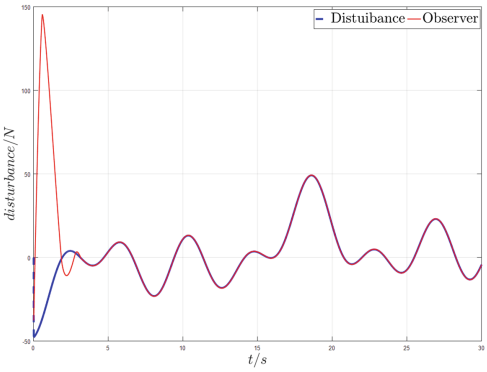

Fig. 2. Observation result of disturbance.

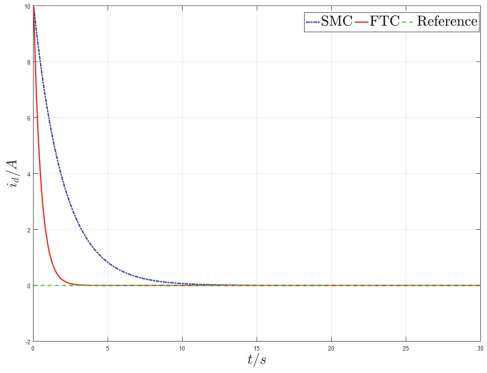

Fig. 3. Desired and actual states for i_d.

the zero vector control strategy, which reduces the reactive power loss of the direct-drive wave power generation system to a certain extent. The active power output of the system is improved. The simulation results are shown in Fig. 4 to 6. Figure 4 shows the tracking results of displacement and velocity and the tracking errors of displacement and velocity under different control strategies. It can be seen that, compared with sliding mode control and backstep sliding mode control, the proposed backstep sliding mode control strategy based on fixed time disturbance observer has smaller tracking error and tracking effect, which ensures that the float is in the running process. It can be in the same direction as the wave excitation force to achieve the purpose of resonance. Figure 5 shows the tracking effect of the q-axis current under three different control strategies. It can be seen that the proposed FTDO-BMSC control strategy can accurately track the reference current due to the interference suppression and compensation brought by the observer. The tracking error is almost zero, so that the back electromagnetic force of the linear generator can be controlled to achieve the condition of maximum power output. Figure 6 shows the energy capture of the

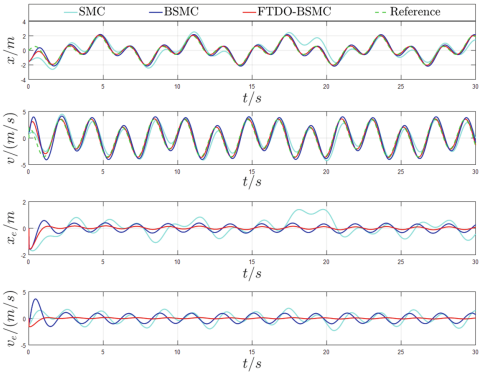

Fig. 4. Desired and actual states for x and v.

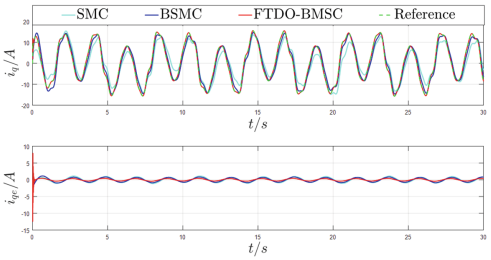

Fig. 5. Desired and actual states for i_q.

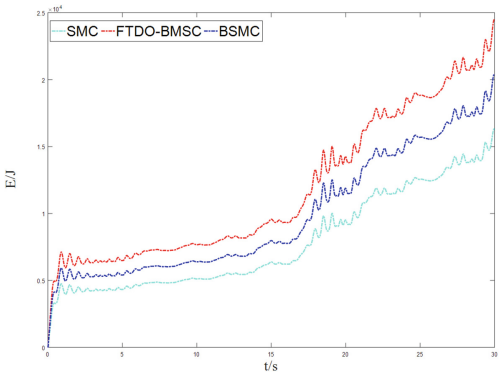

Fig. 6. Wave energy capture results under different control strategies.

direct-drive wave power generation system under different control strategies. It can be seen that compared with the other two control strategies, the proposed method can achieve the maximum wave energy capture, thereby improving the output power, which verifies the effectiveness of the algorithm.

6 Conclusion

In this paper, a backstepping sliding-mode control scheme based on a fixed-time disturbance observer is proposed to solve the power control problem of a direct-drive wave energy conversion (DWEC) under unknown disturbances in actual marine conditions. A fixed-time observer is designed to obser-ve and compensate the disturbance existing in the wave power generation system, which improves the anti-interference of the whole device. A finite-time controller is designed for the d-axis current loop, which reduces the unnecessary power loss of the device and improves the power generation efficiency. A backstepping sliding mode controller is designed for the q-axis current loop to achieve accurate current tracking. In the overall control, the float and the wave achieve the purpose of resonance, and the purpose of maximum power output is achieved. After a rigorous Lyapunov stability analysis, the stability of the entire FTDO-BSMC scheme was proved. The simulation results show the feasibility and effectiveness of the proposed control strategy.

References

1. Lopez, I., Andreu, J., Ceballos, S., Alegria, I.M.D., Kortabarria, I.: Review of wave energy technologies and the necessary power-equipment. Renew Sustain. Energy Rev. **27**, 413–434 (2013)
2. Khan, N., Kalair, A., Abas, N., Haider, A.: Review of ocean tidal, wave and thermal energy technologies. Renew. Sustain. Energy Rev. **72**, 590–604 (2017)
3. Sheng, W.: Wave energy conversion and hydrodynamics modelling technologies: a review. Renew. Sustain. Energy Rev. **109**, 482–498 (2019)
4. Ahamed, R., Mckee, K., Howard, I.: Advancements of wave energy converters based on power take off (PTO) systems: a review. Ocean Eng. **204**, 107248 (2020)
5. de O. Falco, A.F.: Phase control through load control of oscillating-body wave energy converters with hydraulic PTO system. Ocean Eng. **35**(3–4), 358–366 (2008)
6. Henriques, J., Gato, L., Falco, A.F.O., Robles, E., Fa, F.X.: Latching control of a floating oscillating-water-column wave energy converter. Renew. Energy **90**, 229–241 (2016)
7. Teillant, B., Gilloteaux, J.C., Ringwood, J.V.: Optimal damping profiles for a heaving buoy wave energy converter. IFAC Proceed. Vol. **43**(20), 360–365 (2010)
8. Babarit, A., Guglielmi, M., Clement, A.H.: Declutching control of a wave energy converter. Ocean Eng. **36**(12–13), 1015–1024 (2009)
9. Wilson, D.G., Bacelli, G., Robinett, R.D., Korde, U.A., Abdelkhalik, O., Glover, S.F.: Order of magnitude power increase from multi-resonance wave energy converters. In: OCEANS 2017 - Anchorage, pp. 1–7 (2017)
10. Amon, E.A., Brekken, T.K.A., Schacher, A.A.: Maximum power point tracking for ocean wave energy conversion. IEEE Trans. Ind. Appl. **48**(3), 1079–1086 (2012). https://doi.org/10.1109/TIA.2012.2190255
11. Xiao, X., Huang, X., Kang, Q.: A hill-climbing-method-based maximum-power-point-tracking strategy for direct-drive wave energy converters. IEEE Trans. Ind. Electron. **63**(1), 257–267 (2015)
12. Zhao, A., et al.: A flower pollination method based global maximum power point tracking strategy for point-absorbing type wave energy converters. Energies **12**(7), 1343 (2019)

13. Lettenmaier, T., Von Jouanne, A., Brekken, T.: A new maximum power point tracking algorithm for ocean wave energy converters. Int. Jo. Marine Energy **17**, 40–55 (2017)
14. Yue, X., Geng, D., Chen, Q., Zheng, Y., Gao, G., Xu, L.: 2-D lookup table based MPPT: Another choice of improving the generating capacity of a wave power system. Renew. Energy **179**, 625–640 (2021)
15. Valerio, D., Mendes, M.J.G.C., Beirao, P., da Costa, J.S.: Identification and control of the AWS using neural network models. Appl. Ocean Res. **30**(3), 178–188 (2008)
16. Li, L., Wang, H., Gao, Y.: Development of a real-time latching control algorithm based on wave force prediction. IEEE J. Ocean. Eng. **46**(2), 583–593 (2021)
17. Wang, N., Er, M.J., Sun, J.C., Liu, Y.C.: Adaptive robust online constructive fuzzy control of a complex surface vehicle system. IEEE Trans. Cybern. **46**(7), 1511–1523 (2015)
18. Wang, N., Qian, C., Sun, J.C., Liu, Y.C.: Adaptive robust finite-time trajectory tracking control of fully actuated marine surface vehicles. IEEE Trans. Control Syst. Technol. **24**(4), 1454–1462 (2015)
19. Zhan, S., Li, G., Bailey, C.: Economic feedback model predictive control of wave energy converters. IEEE Trans. Ind. Electron. **67**(5), 3932–3943 (2020)
20. Zhan, S., Li, G., Na, J., He, W.: Feedback noncausal model predictive control of wave energy converters. Control. Eng. Pract. **85**(1), 110–120 (2019)
21. Zhan, S., Na, J., Li, G., Wang, B.: Adaptive model predictive control of wave energy converters. IEEE Trans. Sustain. Energy **11**(1), 229–238 (2018)
22. Dalala, Z.M., Zahid, Z.U., Yu, W., Cho, Y.: Design and analysis of an MPPT technique for small-scale wind energy conversion systems. IEEE Trans. Energy Convers. **28**(3), 756–767 (2013)
23. Ybs, A., Ias, B., Al, C.: Smooth second-order sliding modes: Missile guidance application. Automatica **43**(8), 1470–1476 (2007)
24. Wang, N., Su, S.F.: Finite-time unknown observer-based interactive trajectory tracking control of asymmetric underactuated surface vehicles. IEEE Trans. Ind. Inform. **16**(99), 1–10 (2021)
25. Wang, N., Deng, Z.: Finite-time fault estimator based fault-tolerance control for a surface vehicle with input saturations. IEEE Trans. Industr. Inf. **16**(2), 1172–1181 (2020)
26. Wang, N., Er, M.J.: Self-constructing adaptive robust fuzzy neural tracking control of surface vehicles with uncertainties and unknown disturbances. IEEE Trans. Control Syst. Technol. **23**(3), 991–1002 (2014)
27. Wang, N., Karimi, H.R., Li, H., Su, S.F.: Accurate trajectory tracking of disturbed surface vehicles: a finite-time control approach. IEEE/ASME Trans. Mechatron. **24**(3), 1064–1074 (2019)
28. Wang, N., Ahn, C.K.: Coordinated trajectory-tracking control of a marine aerial-surface heterogeneous system. IEEE/ASME Trans. Mechatron. **26**(6), 3198–3210 (2021)
29. Wang, N., Zhang, Y., Ahn, C.K., Xu, Q.: Autonomous pilot of unmanned surface vehicles: Bridging path planning and tracking. IEEE Trans. Veh. Technol. **71**(3), 2358–2374 (2022)
30. Wang, N., Jia, Y., Fu, S.: Spring-resonance-assisted maximal power tracking control of a direct-drive wave energy converter. Trans. Inst. Meas. Control. **43**(13), 3024–3030 (2021)
31. Wang, N., Er, M.J.: Direct adaptive fuzzy tracking control of marine vehicles with fully unknown parametric dynamics and uncertainties. IEEE Trans. Control Syst. Technol. **24**(5), 1845–1852 (2016)